

## Added tables in Supplementary Materials:

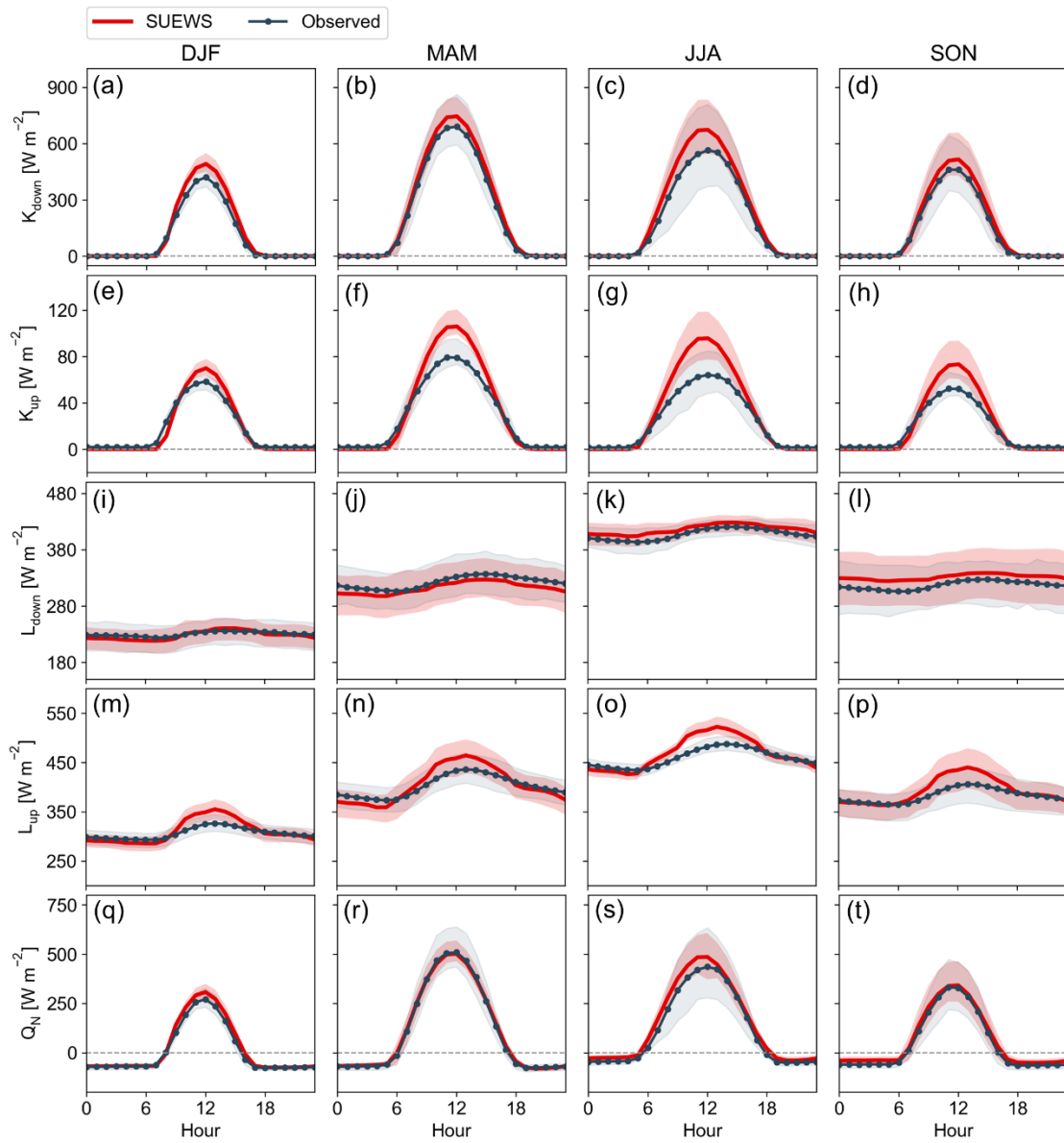
**Table S4.** Adjusted albedo ( $\alpha_i$ ) for different surfaces: buildings (Bldgs), paved surface (Paved), evergreen tree/shrub (Everg), deciduous tree/shrub (Dec), grass, and water following Ward et al (2016). The  $\alpha_i$  for deciduous tree/shrub and grass are allowed to vary from a lower value in summer to a higher value in winter.

	Unit	Bldgs	Paved	Everg	Dec	Grass	Water
$\alpha_i$	–	0.12	0.10	0.10	0.12-0.18	0.18-0.21	0.10

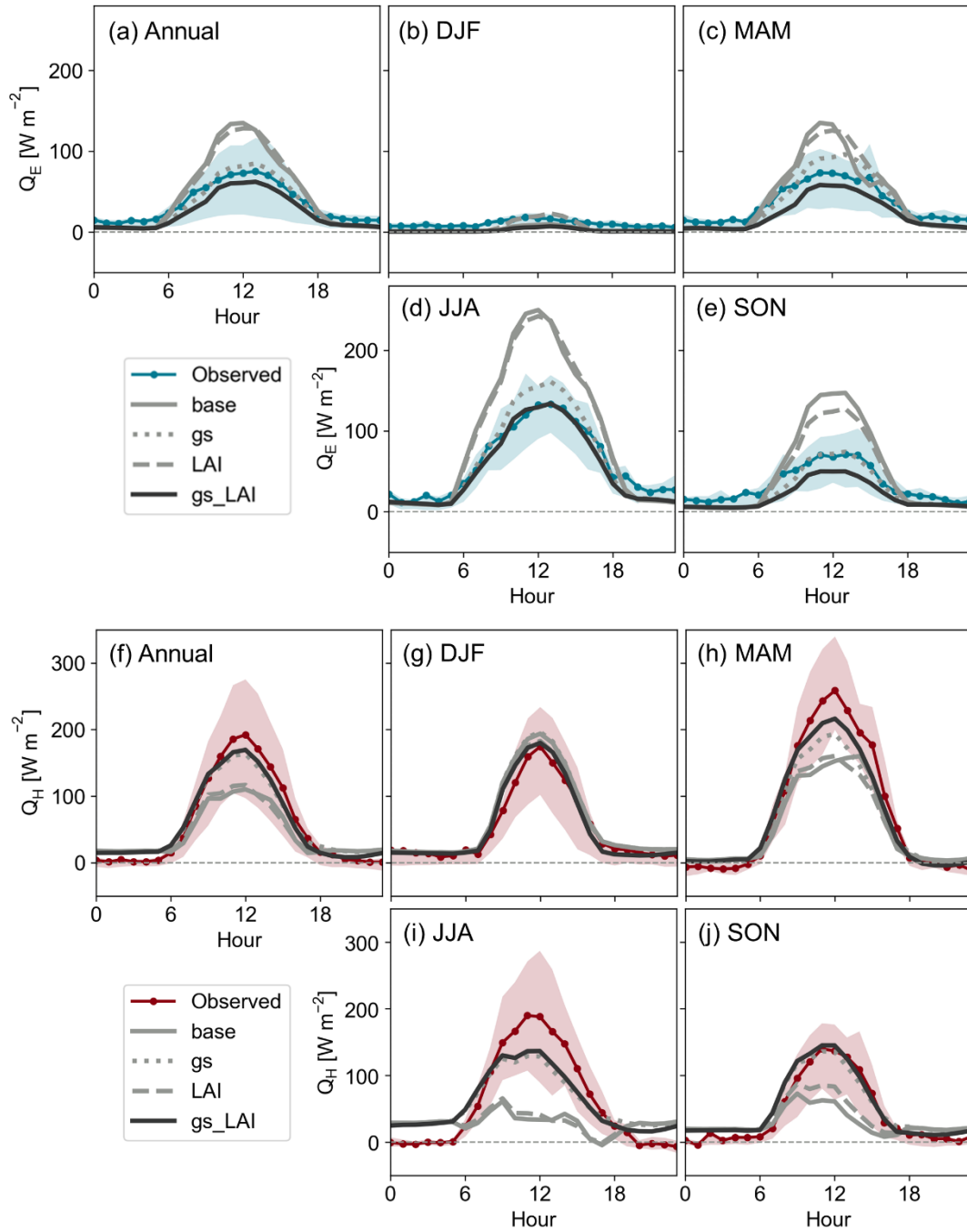
**Table S5.** SUEWS model performance statistics with adjusted albedo ( $\alpha_i$ ) (Table S4) for radiation fluxes, including incoming solar radiation ( $K_{down}$ ), outgoing shortwave radiation ( $K_{up}$ ), incoming longwave radiation ( $L_{down}$ ), outgoing longwave radiation ( $L_{up}$ ), and net radiation ( $Q_N$ ) from May 2010 to June 2011.

	Season	R <sup>2</sup>	RMSE	MBE	N
$K_{down}$	DJF	0.94	52.3	19.5	2160
	MAM	0.93	82.6	19.8	2940
	JJA	0.86	110.4	39.3	2728
	SON	0.93	59.6	16.6	2150
$K_{up}$	DJF	0.88	8.3	-2.5	2160
	MAM	0.92	10.1	0.2	2940
	JJA	0.88	13.6	4.6	2728
	SON	0.91	8.4	0.6	2150
$L_{down}$	DJF	0.74	16.0	-2.4	2160
	MAM	0.86	20.5	-10.0	2940
	JJA	0.68	18.1	8.8	2728
	SON	0.88	23.7	12.9	2150
$L_{up}$	DJF	0.80	15.7	4.0	2160
	MAM	0.90	19.1	3.6	2940
	JJA	0.79	22.5	10.7	2728
	SON	0.90	18.9	9.4	2150
$Q_N$	DJF	0.94	40.5	15.6	2160
	MAM	0.93	64.6	6.0	2940
	JJA	0.86	88.8	32.8	2728
	SON	0.92	51.8	19.5	2150

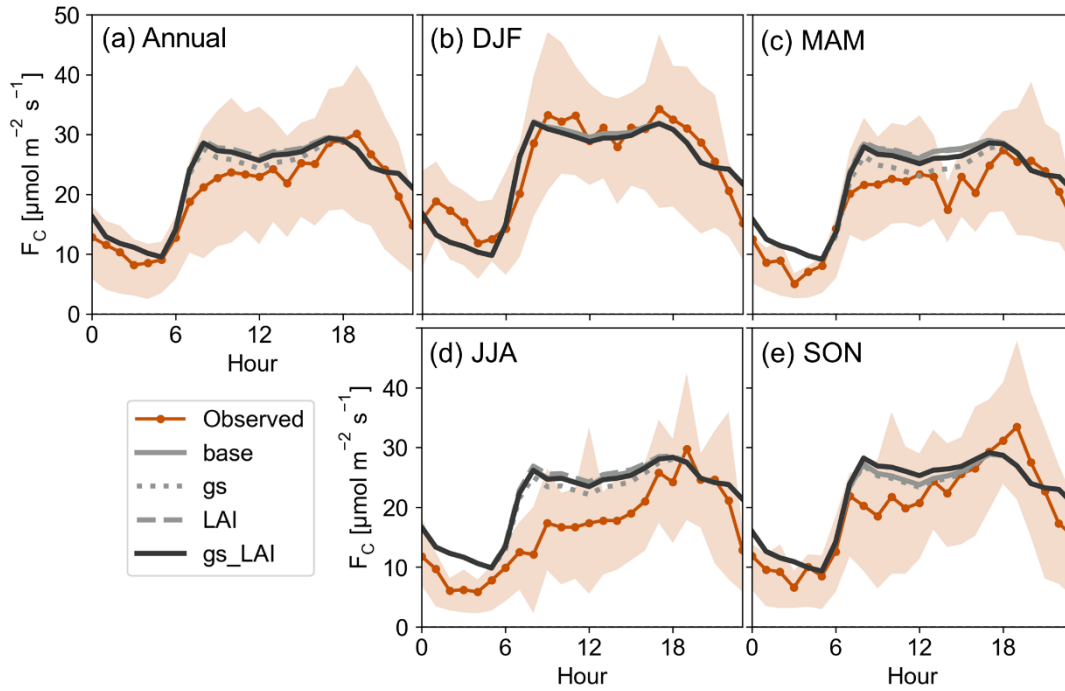
## Modified figures:



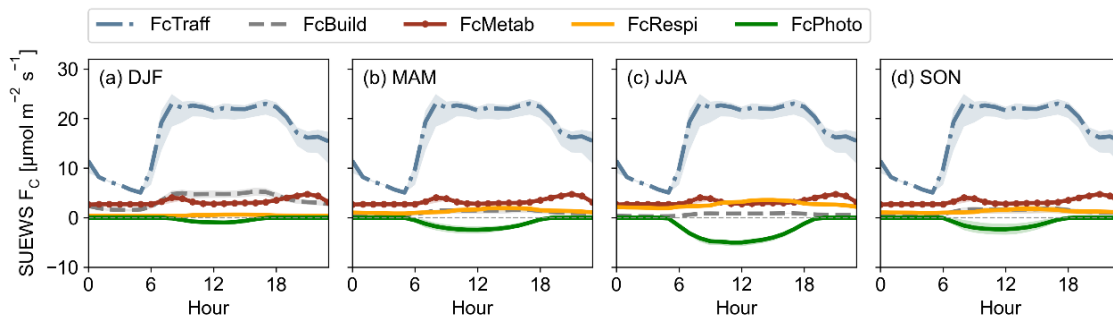
Modified **Figure 5**. Average diurnal cycle of input or modelled and observed hourly radiation fluxes by season, including (a–d) incoming solar radiation ( $K_{down}$ ), (e–h) outgoing shortwave radiation ( $K_{up}$ ), (i–l) incoming longwave radiation ( $L_{down}$ ), (m–p) outgoing longwave radiation ( $L_{up}$ ), and (q–t) net radiation ( $Q_N$ ) from May 2010 to June 2011. Shaded area denotes the interquartile range. Note that only  $K_{down}$  is input and the rest are model output.



Modified **Figure 6**. Annual and seasonal mean diurnal cycles of observed and modelled (a–e) latent heat flux ( $Q_E$ ) and (f–j) sensible heat flux ( $Q_H$ ) for the four model runs (case **base**, **gs**, **LAI**, and **gs\_LAI**) in the year 2016. Shaded area denotes the interquartile range.



Modified **Figure 8**. Annual and seasonal average diurnal cycles of observed and modelled CO<sub>2</sub> flux ( $F_C$ ) for the four model runs (case **base**, **gs**, **LAI**, and **gs\_LAI**) in the year 2016. Shaded area denotes the interquartile range.



Modified **Figure 9**. Seasonal average diurnal cycles of modelled CO<sub>2</sub> flux ( $F_C$ ) components by case **gs\_LAI** in 2016.  $F_C$ Traff denotes  $F_C$  from on-road traffic,  $F_C$ Building building,  $F_C$ Metab human metabolism,  $F_C$ Respi vegetation and soil respiration, and  $F_C$ Photo vegetation photosynthesis. Positive values indicate sources of CO<sub>2</sub> and negative values sinks with respect to the atmosphere. Shaded area denotes the interquartile range.